Involvement of the N- and C-Terminal Fragments of Bovine Pancreatic Deoxyribonuclease in Active Protein Folding†

Wei-Jung Chen,‡ Po-Tsang Huang,‡ Julian Liu,‡ and Ta-Hsiu Liao*,‡,§

Institute of Biochemistry and Molecular Biology, College of Medicine, National Taiwan University, Taipei, Taiwan, and Institute of Biotechnology, College of Bioresources, National Ilan University, Ilan, Taiwan

Received April 23, 2004; Revised Manuscript Received June 21, 2004

ABSTRACT: The three-dimensional structure of bovine pancreatic (bp) DNase revealed that its N- and C-termini form an antiparallel β-sheet structure. The involvement of this β-sheet structure in the active protein folding of bpDNase was thus investigated via a series of deletion and substitution variants. Several substitution variants of N-terminal Leu1 and C-terminal Leu259, and one variant with only the last Thr260 deleted, remained fully active. However, the other deletion variants, in which 2−10 amino acid residues were removed from the C- or N-terminus, all lost the DNase activity. The results indicated that the backbone hydrogen bonding in the antiparallel β-sheet, rather than the side-chain interactions, is crucial for the correct protein folding. When the deletion variants were complemented with synthetic peptides of the deleted N- or C-terminal sequences, the DNase activity was generated. The highest DNase activity was generated when the C-terminal 10-residue-deleted brDNase(Δ251−260) was admixed with the C-terminal 10-residue peptide (peptide C10) in a molar ratio of 1:400. The noncovalent binding between brDNase-(Δ251−260) and peptide C10 exhibited a dissociation constant of 48 μM. Circular dichroism spectra showed that the deletion variants were partially folded with mainly helical structures and that admixture with corresponding peptides facilitated their folding into the nativelike β-sheet-rich structure. Thermal denaturation profiles also revealed that the transition temperature for brDNase(Δ251−260) was increased from 55 to 63 °C after incubation with peptide C10. The folding activation process for the deletion variant occurred in two stages, and Ca^{2+} was required.

Bovine pancreatic deoxyribonuclease I (bpDNase)[1] cleaves double-stranded DNA with no nucleotide sequence specificity (*1*). The enzyme is a compact α,β-protein with approximate dimensions of 45 × 40 × 35 Å (*2*). The chain fold is shown in Figure 1 (*3*). In this three-dimensional structure, the C- and N-termini are in close proximity with the backbone hydrogen bond forming an antiparallel β-sheet structure. Factors contributing to the stability of the enzyme are the intramolecular hydrogen bonds, salt bridges, two disulfide bonds (*4*), and the two structurally bound Ca^{2+} atoms (*5*).

We have previously shown (*6*) that removal of the two C-terminal amino acid residues of bpDNase led to the inactivation of the enzyme, suggesting the critical role of the C-terminal sequence in the final active protein folding. The loss of the DNase activity by removal of the two C-terminal amino acid residues was very likely due to the loss of the stabilizing effect contributed by the antiparallel β-sheet structure. Furthermore, alignment of the N- and C-terminal amino acid sequences of DNases from various species (Figure 2) revealed that residues within the two terminal fragments were well conserved and that most of the polypeptide chains were 260 amino acid residues in length. However, DNases from pig (*7*), dog (*8*), rat (*9*), mouse (*10*), chicken (*11*), and snake (*12*) contained a dipeptide protruding at the C-terminus, while amphibian DNases were characterized by an additional C-terminal fragment of 70 amino acids with a unique cysteine-rich stretch (*13*). Thus, heterogeneity at the C-terminus beyond residue 260 was not an unusual phenomenon among species and probably would not affect the DNase activity.

In the present study, we addressed the important roles of the N- and C-terminal antiparallel β-sheet structure of bpDNase through analyses of a series of substitution and deletion variants. We revealed that formation of the antiparallel β-sheet structure was crucial for the final folded active enzyme. Furthermore, synthetic peptides, whose sequences corresponded to the deleted N- and C-terminal fragments, were able to activate the deletion variants and thus complement the DNase activity. The results indicated that the information necessary for the active folding of bpDNase was written, in part, in the N- and C-terminal sequences. The folding activation process appeared to occur in two stages, and Ca^{2+} was required.

† This work was supported in part by Grant NSC 90-2311-B-002-055 from the National Science Council, Republic of China.

* To whom correspondence should be addressed. Telephone: 886-2-2356-2214. Fax: 886-2-2394-6747. E-mail: thliao@ccms.ntu.edu.tw.

‡ National Taiwan University.

§ National Ilan University.

[1] Abbreviations: bp, bovine pancreatic; br, bovine recombinant; brDNase(WT), recombinant wild-type deoxyribonuclease; brDNase-(Δ*xx*), the N- and C-terminal deletion variants; brDNase(L1X) and brDNase(L259X), the brDNase substitution variants of Leu1 and Leu259, respectively; brDNase(L1X/L259X), doubly substituted variants; SDS, sodium dodecyl sulfate; PAGE, polyacrylamide gel electrophoresis; CD, circular dichroism; TFA, trifluoroacetic acid; T_m, transition temperature; K_d, dissociation constant.

10.1021/bi049183i CCC: $27.50
Published on Web 07/31/2004

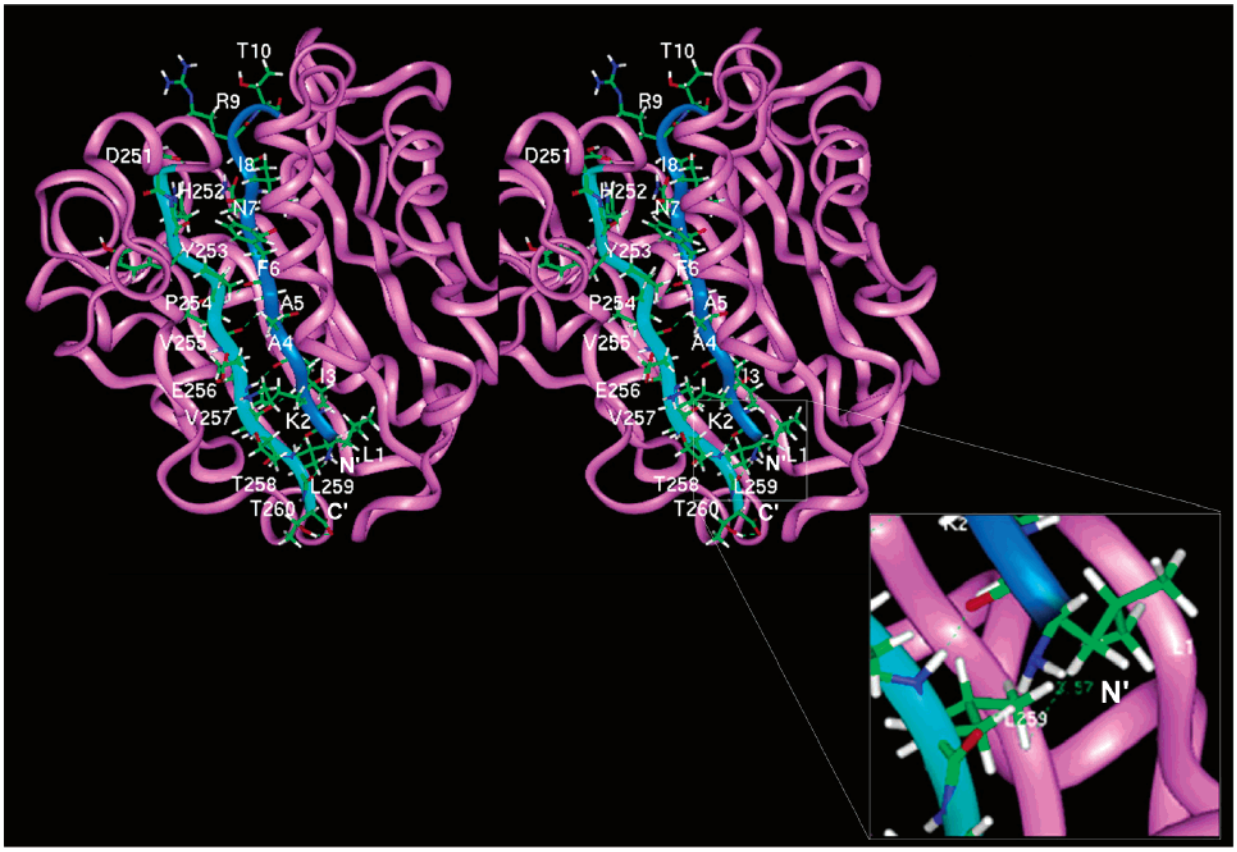

FIGURE 1: Stereoview of the X-ray structure of bpDNase showing the interactions between the N- and C-terminal fragments.The stereo presentation was based on the crystal structure of Oefner and Suck (*3*). The N- and C-terminal antiparallel β-sheet structure was shown with the amino acid side chains. N′ and C′ indicate the N- and C-termini, respectively. Inset: The distance between the side chains of Leu1 and Leu259 is 3.57 (3.6) Å.

	1 10 250 259 260
Bovine	**L**KIAAFNIRT.....SDHYPVEVT**L**T
Ovine	**L**KIAAFNIRT.....SDHYPVEVT**L**T
Porcine	**L**RIAAFNIRT.....SDHYPVEVT**L**KRA
Human	**L**KIAAFNIQT.....SDHYPVEVM**L**K
Canine	**L**RMAAFNIRT.....SDHYPVEVT**L**KRA
Rabbit	**L**KIAAFNIRS.....SDHYPVEVT**L**A
Rat	**L**RIAAFNIRT.....SDHYPVEVT**L**RKT
Mouse	**L**RIAAFNIRT.....SDHYPVEVT**L**RKI
Chicken	**L**RISAFNIRT.....SDHFPVEVT**L**KAR
Snake	**L**RIGAFNIRA.....SDHFPVEVT**L**KST
Frog	**L**KIASFNIQR.....SDHYPVEVE**L**Y.....
Fish	**L**LLGAFNIKS.....SDHFPVEVK**L**S

FIGURE 2: Sequence alignment of the N- and C-terminal fragments of DNases from various species. Sequences were taken from bovine, ovine, porcine (*7*), human (*50*), canine (*8*), rat (*9*), mouse (*10*), rabbit (*51*), chicken (*11*), snake (*12*), frog (*13*), and fish (*52*) DNases. The invariable Leu1 and Leu259 are in bold type.

MATERIALS AND METHODS

Materials. The native bpDNase (code DP) was purchased from Worthington Biochemical Corp. and further purified as previously described (*5*). Calf thymus DNA was obtained from Sigma. All other reagents were of analytical grade.

Site-Directed Mutagenesis. The gene encoding bpDNase has been cloned into pET15b as previously described (*5*). It was used as the wild-type template for site-directed mutagenesis by PCR (*14*) with the synthesized primers. The oligonucleotides used for construction of the brDNase variants were listed in Table S1 (see Supporting Information). The 3′ reverse primers for the C-terminal deletion and Leu259 substitution variants were used with the 5′ forward primer (5′-GCTGG*CCATGG*CCCTGAAGATAG-3′) containing the *Nco*I site. The 5′ forward primers for the N-terminal deletion and Leu1 substitution variants were used with the 3′ reverse primer (5′-CTGGA*CTCGAG*AAGGGACTTATGTC-3′) containing the *Xho*I site. The sequences for the restriction enzyme sites were written in italics. The genes encoding the variants were cloned into the *Nco*I and *Xho*I sites of pET15b. The entire mutated genes were sequenced to confirm the presence of the mutation sites and to ensure no alterations at other sites.

Expression and Purification of the Recombinant Proteins. For protein expression, the plasmids were transformed into the *Escherichia coli* strain BL21(DE3)pLysE. The expressed proteins with DNase activities [brDNase(WT), brDNase(Δ260), brDNase(Δ1), brDNase(L259A), brDNase(L259I), brDNase(L259Y), brDNase(L1D/L259K), and brDNase(L1K/L259D)] caused *E. coli* cells to lyse, resulting in release of the proteins into growth media. After a brief centrifugation of the growth media, the supernatant fractions were used as the sources for a standard purification procedure as previously described (*4*). The cell pellets containing the expressed proteins in inclusion bodies [brDNase(Δ259−260) ∼ brDNase(Δ251−260), brDNase(Δ1−2) ∼ brDNase(Δ1−11), brDNase(L259D), brDNase(L259K), brDNase(L1D), and brDNase(L1K)] were washed extensively and were shown to contain the proteins with purity greater than 95%. The protein purity was checked by SDS−PAGE (*15*) with silver staining (*16*) (Figure 3).

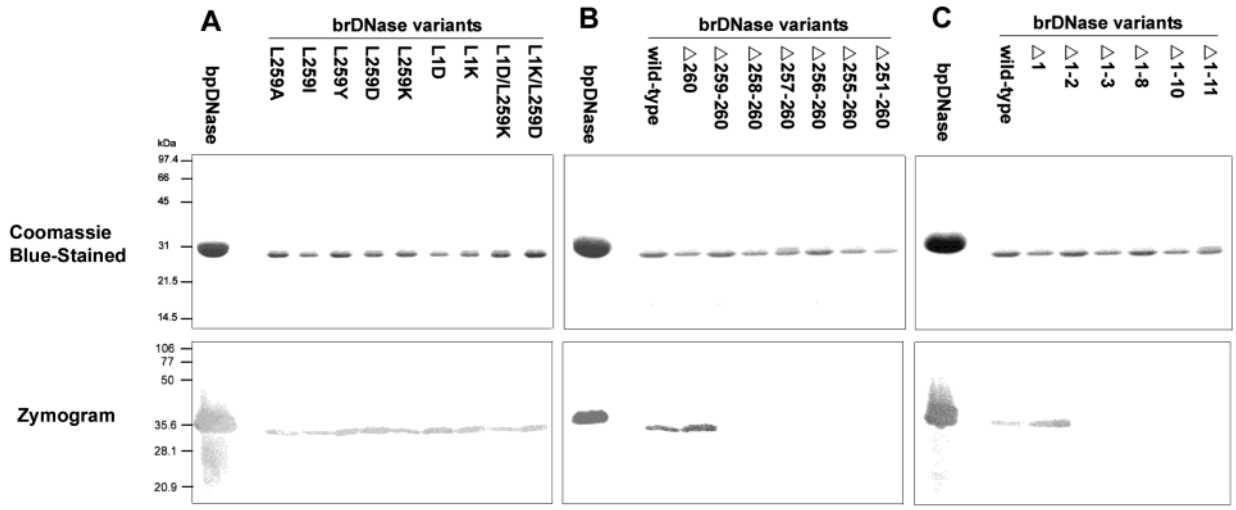

FIGURE 3: SDS−PAGE and zymogram analyses of the purified proteins. (A) The Leu1 and Leu259 substitution variants. (B) The C-terminal deletion variants. (C) The N-terminal deletion variants. Each lane contained 10 μg of total protein. Purified bpDNase was loaded as a control. Upper panel: Coomassie blue-stained gels. Lower panel: zymogram analyses according to Lacks et al. (*53*). All gels were run under nonreducing conditions.

DNase and Protein Assays. The DNase activity was quantitated on the basis of the hyperchromicity due to DNA hydrolysis (*17*). Unless otherwise stated, the assay buffer was 0.1 M Tris-HCl (pH 7.0), containing 10 mM $CaCl_2$, 10 mM $MnCl_2$, and 0.05 mg/mL calf thymus DNA. One unit causes an increase of 1 absorbance unit at 260 nm in 1 mL of assay medium at 25 °C. For calculation of specific activities, the values of protein concentrations were determined using the Bio-Rad protein assay kits (Bio-Rad Laboratories) on the basis of the method of Bradford (*18*) with bovine serum albumin as standard.

Soluble Form of the Recombinant Proteins Obtained from Inclusion Bodies. The pellets of the recombinant proteins in the inclusion bodies were normally dissolved in 6 M guanidine hydrochloride and then dialyzed against a Ca^{2+}-containing buffer (10 mM Tris-HCl, pH 7.0) to remove the denaturing agent. The proteins thus treated were soluble. However, when the pellets were dissolved in 6 M guanidine hydrochloride and then dialyzed against the Ca^{2+}-free buffer, the proteins were precipitated. To obtain a soluble form in the Ca^{2+}-free buffer, we employed a lower concentration of the protein (0.1 mg/mL) and a higher pH (pH 8.5) dialysis buffer at the beginning and then gradually decreased to pH 7.0. By this manner, little precipitate was observed, and the solutions were used directly for further studies.

CD Measurements. Unless otherwise stated, all of the CD measurements were carried out at room temperature using a Jasco J-715 spectropolarimeter with a 1 mm optical path cell over a range of 190−260 nm, with 1 s response time and 20 nm/min scan speed. All spectra were the average of five scans at an interval of 1 nm. Prior to calculation of the final ellipticity, all spectra were smoothed and corrected for buffer blanks. In peptide complementation experiments, all spectra were further corrected by subtracting the peptide reference spectra. The CD intensities are expressed as molar ellipticities (deg cm^2 $dmol^{-1}$). The percentage of secondary structures was calculated using the method of Wu et al. (*19*) and Chen et al. (*20*).

Chemical Synthesis of Peptides. The peptides for complementation studies [peptide N6, LKIAAF (661.84 Da); peptide N10, LKIAAFNIRT (1146.40 Da); peptide C6, VEVTLT (660.77 Da); peptide C10, DHYPVEVTLT (1173.29 Da); peptide C10A, DAYPVEVTLT (1107.23 Da)] were synthesized on a solid-phase peptide synthesizer (Model 433A; Applied Biosystems). The C-terminal Fmoc amino acid for each peptide was loaded on a hydroxymethyl resin (Wang resin, 1.0 mmol/g substitution) using the dicyclohexylcarbodiimide/4-(*N*,*N*′-dimethylamino)pyridine strategy in dichloromethane. Capping was accomplished with acetic anhydride in the presence of diisopropylethylamine. Single coupling was carried out for each residue using the FastMoc chemistry (HBTU/HOBt activation strategy). The resin weight gain was 70−80% relative to the theoretical. For the cleavage of peptide N10, a solution containing 0.75 g of phenol, 0.5 mL of H_2O, 0.5 mL of thioanisole, 0.25 mL of ethylethanedithiol, and 10 mL of TFA was used. For the cleavage of the rest of the peptides, the standard solution of 95% TFA was employed. The crude peptides were separated from the resin by filtration with glass funnels. The filtrates were reduced to a small volume with a rotary evaporator. The peptides were precipitated from diethyl ether and lyophilized to yield white solid powders. The purity of the peptides was checked by reversed-phase HPLC with a linear gradient of water (0.1% TFA)−80% acetonitrile (0.08% TFA). The amino acid analyses of the peptides, as described previously (*4*), were carried out to further confirm the purity. The resulting peptides were used directly since the purity was greater than 95%.

RESULTS

The Leu1 and Leu259 Substitution Variants. The intramolecular contact distance between the side chains of Leu1 and Leu259 was 3.6 Å (Figure 1, inset), and their backbone had main-chain hydrogen bonding within the N- and C-terminal antiparallel β-sheet structure. Because Leu1 and Leu259 were invariable in the sequence alignment (Figure 2) and removal of the C-terminal Leu-Thr dipeptide caused the loss of the DNase activity (*6*), we thus investigated the degree of involvement of Leu1 and Leu259 in the final folding of bpDNase through a series of substitution variants.

Three of the C-terminal substitution variants [brDNase-(L259A), brDNase(L259I) and brDNase(L259Y)], expressed

Table 1: Activities of bpDNase and the Active brDNase Variants

DNase form	DNase activity[a] (units/mL)	protein concn (mg/mL)	specific activity (units/mg)	expressed protein in[b]
bpDNase	207.7 ± 2.1	0.213	975.0 ± 9.6	tissue
brDNase(Δ260)	145.0 ± 2.8	0.169	858.6 ± 8.7	media
brDNase(Δ1)	128.0 ± 3.5	0.138	926.7 ± 12.4	media
brDNase(L259A)	120.7 ± 2.5	0.129	935.4 ± 19.3	media
brDNase(L259I)	136.7 ± 1.2	0.141	969.3 ± 8.8	media
brDNase(L259Y)	142.7 ± 2.5	0.148	964.0 ± 16.9	media
brDNase(L259D)	94.0 ± 4.5	0.120	783.3 ± 37.9	inclusion bodies
brDNase(L259K)	83.7 ± 2.9	0.098	853.7 ± 29.3	inclusion bodies
brDNase(L1D)	105.0 ± 0.8	0.124	846.8 ± 6.6	inclusion bodies
brDNase(L1K)	113.7 ± 2.6	0.135	842.0 ± 19.4	inclusion bodies
brDNase(L1D/L259K)	176.7 ± 3.4	0.197	896.8 ± 17.3	media
brDNase(L1K/L259D)	159.7 ± 2.9	0.166	961.8 ± 17.3	media

[a] The DNase activity was expressed as the average of triplicates. [b] The proteins expressed in the inclusion bodies (2.5−6 μg) were dissolved in 20 μL of 6 M guanidine hydrochloride and then diluted 10-fold into 100 mM Tris-HCl (pH 7.0) containing 10 mM $CaCl_2$. After 1 h, a 10 μL aliquot of the diluted solution was removed for measurement of DNase activity using the hyperchromicity assay.

in the growth media, were fully active (Table 1). The other two variants [brDNase(L259D) and brDNase(L259K)], albeit expressed in the inclusion bodies, were DNase active as evidenced by zymogram analyses (Figure 3A) and were able to generate 80−87% of DNase activities (Table 1). The two N-terminal substitution variants of Leu1 [brDNase(L1D) and brDNase(L1K)] were also expressed in the inclusion bodies. Similar to their Leu259 counterparts, both were DNase active by zymogram analyses (Figure 3A) and had 86−87% of DNase activities as measured by the hyperchromicity assay (Table 1).

An assessment of the side-chain interactions between Leu1 and Leu259 was obtained from two doubly mutated variants [brDNase(L1D/L259K) and brDNase(L1K/L259D)] with the side-chain charge-to-charge attraction. The two variants were almost fully active by the hyperchromicity assay (Table 1) and were shown to be DNase active by zymogram analyses (Figure 3A). To gain further insight into the effect of the side-chain interactions between Leu1 and Leu259 in bpDNase, we performed thermal stability studies on the substitution variants. As shown in Figure 4, the brDNase(L259D) and brDNase(L1K) variants, each with a substituted charged residue, were inactivated at a T_m of 60 °C in contrast to 66 °C for the native bpDNase. The decreased transition temperature indicated that the substitution of a hydrophobic with a polar residue reduced the protein stability. On the other hand, a T_m of 65−66 °C for the two doubly mutated variants [brDNase(L1D/L259K) and brDNase(L1K/L259D)] revealed that the charge-to-charge attraction could contribute to the protein stability. It is thus concluded that the side-chain interaction between Leu1 and Leu259, though affecting the initial protein folding and resulting in the inclusion bodies, has no effect in achieving the final active enzyme folding from the 6 M guanidine hydrochloride-dissolved proteins.

The Deletion Variants. The C-terminal sequence crucial for the activity of bpDNase (*6*) was previously shown by

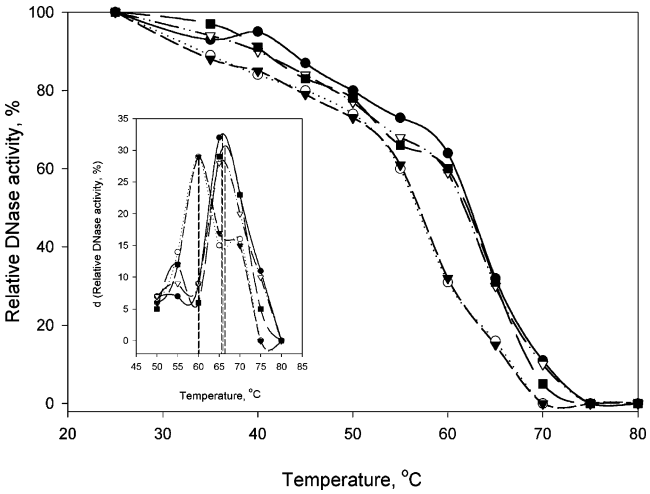

FIGURE 4: Thermal inactivation profiles for the substitution variants. The purified bpDNase or a recombinant protein in a 20 mM Tris-HCl (pH 7.5) buffer containing 10 mM $CaCl_2$ was heated at the specified temperature for 10 min and cooled immediately on ice. DNase activities were then measured using the hyperchromicity assay with an estimated error of 5%. Inset: First derivative of the relative DNase activities for locating T_m. Symbols: ●, bpDNase; ○, brDNase(L259D); ▼, brDNase(L1K); ▽, brDNase(L1D/L259K); ■, brDNase(L1K/L259D).

the removal of the C-terminal amino acid residues with carboxypeptidase A. In the present study, we also obtained similar information through a series of C-terminal deletion variants. The brDNase(Δ260), losing only the last Thr260, remained active (Table 1). However, the expressed proteins of other deletion variants, with the polypeptide chains 2−10 amino acid residues shorter, were found in the inclusion bodies and were not DNase active as shown by zymogram analyses (Figures 3B).

The hypothesis that both N- and C-terminal fragments were involved in the stabilization of the DNase molecule was confirmed by another deletion series of the N-terminus. Except for brDNase(Δ1) with almost full DNase activity as measured by the hyperchromicity assay (Table 1) and as evidenced by zymogram analysis (Figure 3C), the rest of the deletion variants were all expressed in the inclusion bodies and were not DNase active (Figure 3C). Because the 5′ forward primer was designed to contain the restriction site of *Nco*I (CCATGG), a Met-Ala dipeptide was thus added to the N-terminus of the biosynthesized polypeptide chain. To acknowledge the final protein obtained, we subjected the recombinant proteins to N-terminal protein sequence analyses. Three of the purified N-terminal deletion variants [brDNase(Δ1), brDNase(Δ1−3), and brDNase(Δ1−8)] all showed PTH-Ala with quantitative yields in the first Edman degradation cycle (data not shown). Thus, the N-terminal first amino acid residue fMet was essentially removed in all instances during or after the polypeptide was synthesized in *E. coli*. With Ala as the new N-terminal residue, brDNase(Δ1) was actually brDNase(L1A), and brDNase(Δ1−2) should be brDNase(Δ1/K2A), and presumably the rest of the N-terminal variants had Ala as the N-terminus. The fact that brDNase(L1A) was fully active while the DNase activity was completely lost in brDNase(Δ1/K2A) indicated that the backbone hydrogen bonding in the N- and C-terminal antiparallel β-sheet structure, rather than the side-chain interactions between Leu1 and Leu259, is crucial for the correct folding.

Peptide Complementation. The C-terminal 10-residue-deleted variant [brDNase(Δ251−260)] was not DNase active (Figure 5A) using the hyperchromicity assay and as shown by zymogram analyses (Figure 3B). When this deletion variant was incubated with the C-terminal 10-residue peptide (peptide C10), DNase activities were generated and increased with time, reaching a plateau at about 8 h (Figure 5A). The saturation profile (Figure 5B) exhibited a maximum activation at approximately 80 μM (400 equiv) peptide C10, and a double reciprocal plot was obtained from the same data and was used to obtain K_d (Figure 5B, inset). The maximum recoverable DNase activities and K_d for all of the deletion variant−synthetic peptide complexes were summarized in Table 2. Among all of the combinations, peptide C10 interacting with the brDNase(Δ251−260) variant had the lowest K_d of 48 μM. Peptide C6, missing the catalytic residue His252 (*21*), was unable to generate the DNase activity with brDNase(Δ251−260). Peptide N6, without the substrate binding residue Arg9 (*22*), was also unable to generate the DNase activity with brDNase(Δ1−10) or brDNase(Δ1−11).

As shown in Figure 5A, the formation of the brDNase-(Δ251−260)−peptide C10 complex was a slow process in a time scale of hours, suggesting a likely involvement of protein conformational changes. To determine whether such changes could be reversed, they were subjected to the studies of the dissociation kinetics of the complex. Figure 5C showed that the dissociation of peptide C10 from the complex was indeed slow as well. The $t_{1/2}$ for the dissociation was calculated to be approximately 6.9 min.

CD Spectra. The CD spectrum (Figure 6A) of the native bpDNase showed a broad minimum centered at about 215 nm and a strong positive maximum at 198 nm with a crossover point at 204 nm, indicating the presence of mainly a β-sheet conformation. Similar CD spectra were observed in brDNase(WT) and the active, single amino acid deleted brDNase(Δ260) variant (Figure 6A) as well as all of the active Leu1 and Leu259 substitution variants (data not shown). When the polypeptide chains were further shortened with loss of DNase activities, their CD spectra (Figure 6A) displayed an intense negative maximum at 208 nm, a weak negative band at 220 nm, and a positive band at 193 nm, showing an apparent increase in α-helix and random structure accompanied by a decrease in β-sheet and turn structure. On the basis of the CD spectra, the percentages of secondary structures for all the deletion and substitution variants were calculated and summarized in Table 3. The estimated amounts of the secondary structure for all of the Leu1 and Leu259 substitution variants were very similar to those of the native bpDNase.

The 10-residue-deleted variant, brDNase(Δ251−260), by itself, displayed a CD spectrum of a double minimum at 208 and 220 nm and a positive band at 193 nm, a characteristic of an α-helix-rich conformation (Figure 6B). Upon incubation with the 10-residue peptide C10 for more than 4 h, the two distinct bands at 208 and 220 nm changed into one broad negative trough centered at 215 nm, and a positive band shifted to 198 nm with increasing crossover points from 200 to 204 nm. These spectral changes indicated that the structure of the deletion variant, upon peptide C10 binding, shifted into a conformation with more β-sheets accompanied by reduction of either random or helical contents. Similar changes also took place when the N-terminal deletion variant,

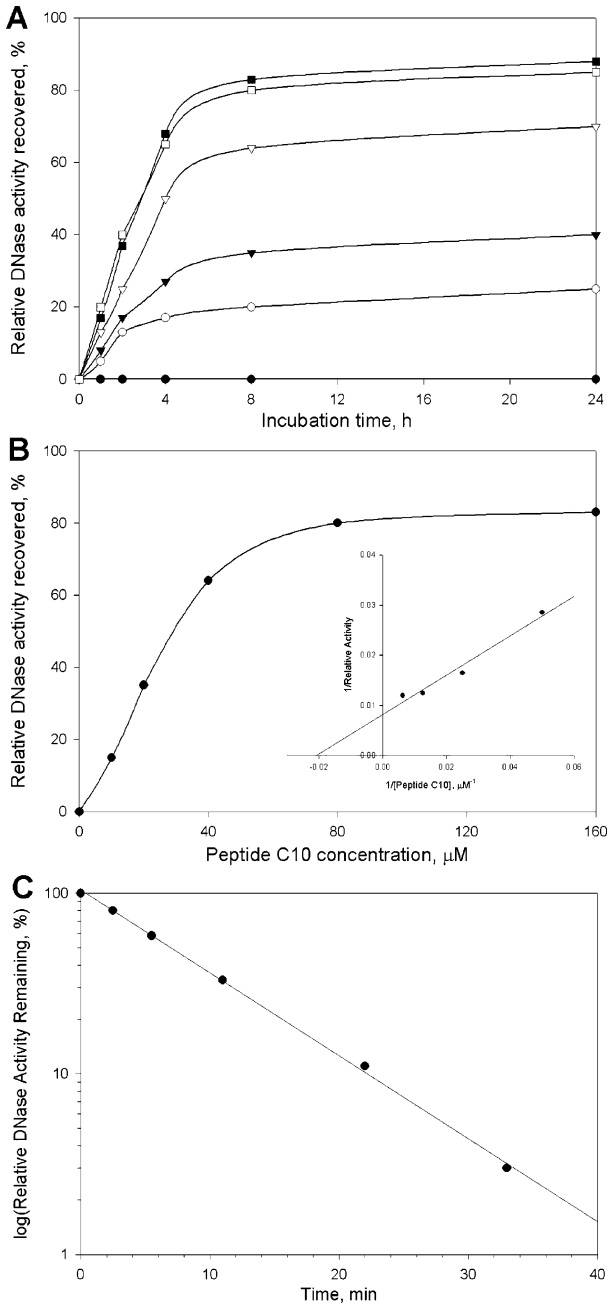

FIGURE 5: Kinetic and saturation profiles for the brDNase(Δ251−260) variant complemented with peptide C10. All DNase activities were measured using the hyperchromicity assay. (A) Kinetics for the interaction between brDNase(Δ251−260) and peptide C10. The brDNase(Δ251−260) variant (0.2 μM) in 20 mM Tris-HCl (pH 7.5) containing 10 mM Ca^{2+} was incubated at room temperature with peptide C10. At selected time intervals, an aliquot was removed and assayed for DNase activities. Concentrations of peptide C10: ●, 0 μM; ○, 10 μM; ▼, 20 μM; ▽, 40 μM; ■, 80 μM; □, 160 μM. (B) The saturation curve for peptide C10. Various concentrations of peptide C10 were incubated with 0.2 μM brDNase(Δ251−260) at room temperature for 8 h and then assayed for DNase activities. Inset: the double reciprocal plot for calculation of K_d. (C) Dissociation kinetics for the brDNase(CΔ251−260) variant−peptide C10 complex. The brDNase(Δ251−260) variant (0.2 μM) was incubated with peptide C10 (80 μM) for 8 h, and then the mixture (100 μL) was placed through a Sephadex G-25 column (0.5 × 6 cm). Fractions of 50 μL were collected, and the fraction showing the highest DNase activity was selected and assayed for DNase activities at the various time intervals. The time shown in the figure included the lagging time required to reach the slope for measuring the DNase activity (0.5−1.5 min). Time zero was the time when the sample was applied onto the column.

Table 2: Maximum Recoverable DNase Activity and K_d for the Peptide−brDNase Variant Complexes[a]

	peptide C10 (DHYPVEVTLT)		peptide C6 (VEVTLT)			peptide N10 (LKIAAFNIRT)		peptide N6 (LKIAAF)			peptide C10A (DAYPVEVTLT)	
recombinant protein	max recov DNase act. (%)	K_d (μM)	max recov DNase act. (%)	K_d (μM)	recombinant protein	max recov DNase act. (%)	K_d (μM)	max recov DNase act. (%)	K_d (μM)	recombinant protein	max recov DNase act. (%)	K_d (μM)
brDNase(Δ259−260)	10	103	3	275	brDNase(Δ1−2)	10	134	4	164	brDNase (Δ251−260)	no DNase activity	
brDNase(Δ258−260)	17	90	5	148	brDNase(Δ1−3)	15	118	5	139			
brDNase(Δ257−260)	25	86	8	87	brDNase(Δ1−8)	72	76	11	113			
brDNase(Δ256−260)	48	59	10	80	brDNase(Δ1−10)	83	68	0	ND			
brDNase(Δ255−260)	67	52	17	54	brDNase(Δ1−11)	88	57	0	ND			
brDNase(Δ251−260)	83	48	0	ND[b]								

[a] The reaction mixture containing 0.2 μM brDNases and 0−160 μM synthetic peptides in 100 mM Tris-HCl (pH 7.0) was incubated at room temperature for 8 h and assayed for DNase activities. Plots such as Figure 5B for the other variants were also obtained to calculate the rest of the values, including K_d. [b] ND, not determined.

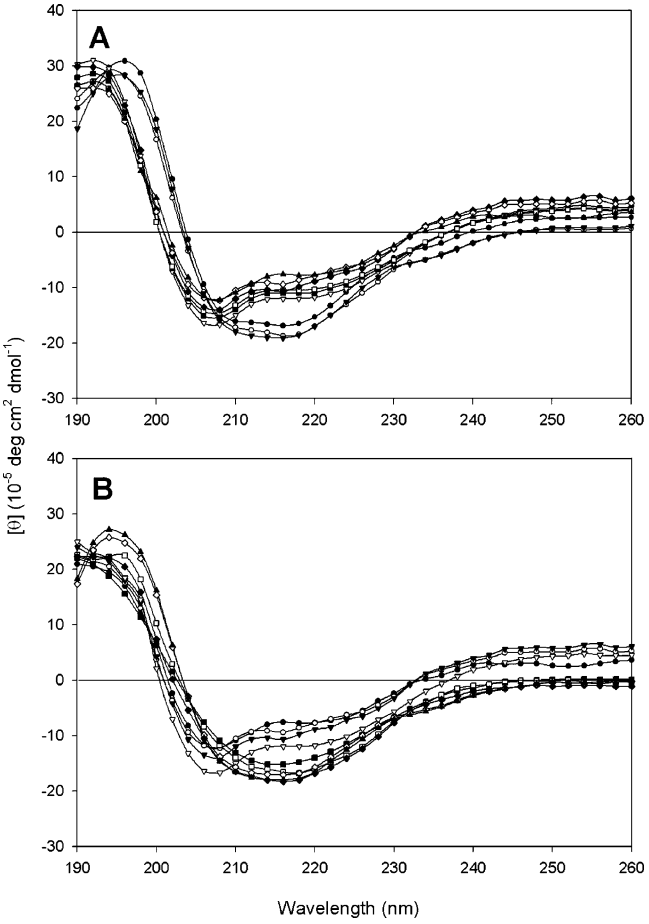

FIGURE 6: CD spectra for bpDNase and the recombinant proteins. All of the spectra were collected with 3.5−4.0 μM proteins in 10 mM Tris-HCl, pH 7.0, containing 10 mM Ca^{2+}. (A) Spectra: ●, bpDNase; ○, brDNase(WT); ▼, brDNase(Δ260); ▽, brDNase(Δ259−260); ■, brDNase(Δ258−260); □, brDNase(Δ257−260); ◆, brDNase(Δ256−260); ◇, brDNase(Δ255−260); ▲, brDNase(Δ251−260). (B) The brDNase(Δ251−260) variant complemented with peptide C10 (500 μM). Spectra: ●, brDNase(Δ251−260); after addition of peptide C10 for ○, 10 min; ▼, 20 min; ▽, 30 min; ■, 1 h; □, 2 h; ◆, 4 h; ◇, 8 h; ▲, 24 h.

brDNase(Δ1−11), was complemented with the N-terminal 10-residue peptide N10 (data not shown).

When the deletion variant, brDNase(Δ251−260), was incubated for 24 h with 400 equiv of peptide C10A (a peptide in which the catalytically essential His residue in peptide C10 was replaced by Ala), no activation was observed (Table 2). However, the CD spectra (data not shown) revealed that the protein structure shifted into a conformation with more β-sheets, 4 h after addition of peptide C10A, suggesting that peptide C10A was bound to the deletion variant but without the DNase activity.

Table 3: Percentages of Secondary Structures in bpDNase and the brDNase Variants Based on CD Measurements

DNase form	α-helix (%)	β-sheet (%)	turn (%)	random (%)	DNase
bpDNase-3D[a]	29	51	14	6	
bpDNase	36	55	6	3	active
brDNase(WT)	34	54	9	3	active
brDNase(Δ260)	35	53	8	4	active
brDNase(Δ259−260)	41	34	8	17	inactive
brDNase(Δ258−260)	44	33	5	18	inactive
brDNase(Δ257−260)	45	32	5	18	inactive
brDNase(Δ256−260)	48	30	3	19	inactive
brDNase(Δ255−260)	49	29	4	19	inactive
brDNase(Δ251−260)	55	24	1	20	inactive
brDNase(Δ1)	33	54	6	7	active
brDNase(Δ1−2)	40	35	6	19	inactive
brDNase(Δ1−3)	42	35	4	17	inactive
brDNase(Δ1−8)	47	30	5	19	inactive
brDNase(Δ1−10)	52	25	4	19	inactive
brDNase(Δ1−11)	53	23	4	20	inactive
brDNase(L259A)	35	51	9	5	active
brDNase(L259I)	36	51	8	5	active
brDNase(L259Y)	36	50	9	5	active
brDNase(L259D)	38	46	10	6	active
brDNase(L259K)	38	46	11	5	active
brDNase(L1D)	39	46	10	5	active
brDNase(L1K)	39	47	10	5	active
brDNase(L1D/L259K)	35	51	11	3	active
brDNase(L1K/L259D)	34	51	10	4	active

[a] The secondary structure content was derived from the crystal structure of bpDNase (RCSB Protein Data Bank ID 3DNI).

Thermal Stability. Thermal denaturation profiles (Figure 7) showed a T_m of 65 °C for bpDNase and only 55 °C for the deletion variant, brDNase(Δ251−260), suggesting that removal of the last 10 amino acid residues had a great effect on the thermal stability. However, when brDNase(Δ251−260) was incubated with peptide C10, a shift of T_m from 55 to 63 °C was observed, indicating the increase of protein stability upon peptide binding.

Role of Ca^{2+} in the Folding Activation Process. Two calcium atoms play a structural role in bpDNase (*3*), and Ca^{2+} is required for the active conformation (*5*). Calcium ions can protect bpDNase from inactivation by β-mercaptoethanol

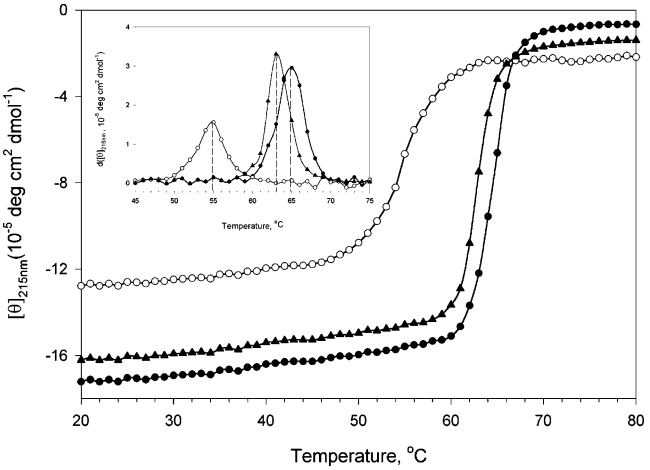

FIGURE 7: Thermal denaturation profiles for peptide complementation. The CD of the proteins (4.5 μM) in 10 mM Tris-HCl (pH 7.0) containing 10 mM Ca^{2+} was monitored at 215 nm. The temperature was increased at a rate of 1.0 °C/min using a jacketed cell of 1 mm optical path length. For peptide complementation, 4.5 μM proteins and 500 μM peptides were incubated at room temperature for 20 h prior to heating. Symbols: ●, bpDNase; ○, brDNase-(Δ251−260); ▲, brDNase(Δ251−260) complemented with peptide C10. Inset: The first derivative of the three curves to locate T_m.

(*23*) or proteases (*24*) and can induce a significant amount of conformational (*25*) and hydrodynamic changes (*26*). Thus, Ca^{2+} plays an important role in not only the protein structure but also the DNase activity. Therefore, understanding the Ca^{2+} involvement in the folding activation of the deletion variants with the complementary peptides is of equal importance.

The CD spectrum (Figure 8A) of brDNase(Δ251−260) in a Ca^{2+}-free buffer showed an intense negative peak around 200 nm, typical of a random coil structure, indicating that the recombinant protein without Ca^{2+} was in an unfolded conformation. However, when Ca^{2+} was added, a rapid folding was observed within 2 min with a CD spectrum displaying a structure rich in α-helix. This spectrum was very similar to that obtained from brDNase(Δ251−260) in the Ca^{2+}-containing buffer (Figure 8A). After incubation for more than 4 h with Ca^{2+}, admixture with peptide C10 further facilitated the folding of the protein into a mainly β-sheet structure with DNase activity. Moreover, the thermal denaturation profile of brDNase(Δ251−260) in the Ca^{2+}-free buffer, monitored by the CD signal (Figure 8B), showed a gradual change without a sharp transition temperature, indicative of a structure with random coils.

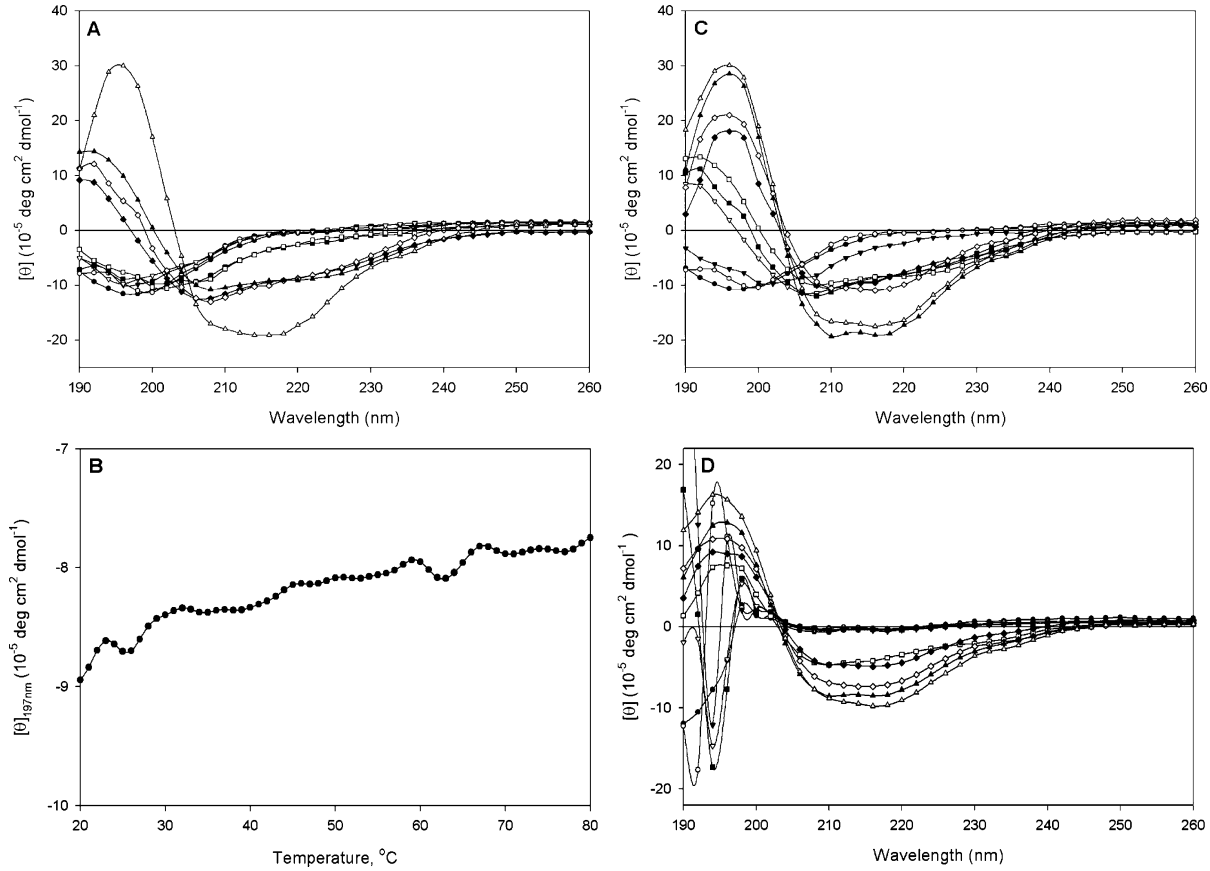

FIGURE 8: Role of Ca^{2+} in the folding activation process. The buffer referred to is 10 mM Tris-HCl, pH 7.0. (A) CD spectra: ●, brDNase-(Δ251−260) in the Ca^{2+}-free buffer; ○, 35 s after addition of 10 mM Ca^{2+}; ▼, 50 s after; ▽, 65 s after; ■, 80 s after; □, 95 s after; ◆, 110 s after; ◇, 125 s after; ▲, 140 s after; △, 4 h after an extra addition of peptide C10 (500 μM). (B) Thermal denaturation profile for brDNase(Δ251−260) in the Ca^{2+}-free buffer. Data were collected by monitoring the CD signal at 197 nm. (C) CD spectra for brDNase-(Δ251−260) upon incubation with peptide C10 followed by the addition of 10 mM Ca^{2+}. Symbols: ●, in the Ca^{2+}-free buffer and without peptide C10; ○, 4 h after addition of peptide C10 (500 μM); ▼, 1 min after an extra addition of 10 mM Ca^{2+}; ▽, 2.5 min after; ■, 10 min after; □, 30 min after; ◆, 1 h after; ◇, 2 h after; ▲, 4 h after; △, 8 h after. (D) CD spectra for bpDNase: ●, in the Ca^{2+}-free buffer; ○, 30 s after addition of 10 mM Ca^{2+}; ▼, 1 min after; ▽, 2 min after; ■, 5 min after; □, 10 min after; ◆, 20 min after; ◇, 30 min after; ▲, 40 min after; △, 60 min after. The bpDNase in the Ca^{2+}-free buffer was prepared by dissolving the purified bpDNase (45 μg) in 300 μL of 6 M guanidine hydrochloride and then dialyzed against the Ca^{2+}-free buffer.

When peptide C10 was added to brDNase(Δ251−260) in the Ca^{2+}-free buffer, the CD spectrum of random coils remained unchanged for 4 h, indicating no interactions between the protein and the peptide. When 10 mM Ca^{2+} was then added to the same reaction mixture, a folding process was observed, as evidenced by the CD spectrum (Figure 8C). These observations suggested that the deletion variant, probably with the assistance of Ca^{2+}, folded to a helix-rich structure rapidly within 2 min and then slowly folded to the mainly β-sheet structure after peptide C10 binding.

Whether the folding pathway involving Ca^{2+} is the same for the truncated polypeptide of the deletion variant as for the intact polypeptide of bpDNAse must be answered in order to gain a full understanding of the active protein folding. Thus, bpDNase (0.1 mg/mL) was first denatured in 6 M guanidine hydrochloride and then dialyzed against a Ca^{2+}-free buffer (10 mM Tris-HCl, pH 7.0) to remove the denaturant. As shown in Figure 8D, the CD spectra for this Ca^{2+}-free, denatured bpDNase displayed an intense negative maximum around 193 nm, a small positive signal at 198 nm, and a minor broad negative trough between 210 and 220 nm with a crossover point at 204 nm, indicating a turn-rich structure with some β-pleated sheets. According to the secondary structure estimation, the structure consisted of 45% turn, 35% β-sheet, 17% random coil, and an unusually low helix content of 3%. These observations indicated that the denatured bpDNase was unable to refold back to the correct conformation without the assistance of Ca^{2+}, and this misfolded protein was inactive as assayed with the hyperchromicity assay. However, when 10 mM Ca^{2+} was added back, the CD spectrum exhibited significant increases in both the α-helix and β-sheet structures after 10 min, with about 15% reactivation of the DNase activity. After 1 h, the CD spectrum of the estimated secondary structures returned to that of the native bpDNase with 85% DNase activity.

DISCUSSION

For clarity, the critical roles of Ca^{2+} in the folding activation of the deletion variant, brDNase(Δ251−260), by peptide C10 as well as the refolding of the guanidine hydrochloride-denatured bpDNase to the active conformation are summarized and presented as schemes (see Figure 9). In Scheme I, brDNase(Δ251−260) in a Ca^{2+}-free buffer was in an unfolded conformation, and upon Ca^{2+} addition, a partially folded structure rich in α-helix was formed. Incubation with peptide C10 further facilitated the folding of the polypeptide to a mainly β-sheet structure with DNase activity. However, when peptide C10 was added to brDNase(Δ251−260) in the Ca^{2+}-free buffer, the unfolded structure remained unchanged because there were no interactions between the protein and peptide C10. However, upon Ca^{2+} addition, the deletion variant, probably with the assistance of Ca^{2+}, rapidly folded to a helix-rich structure and then slowly folded to the mainly β-sheet structure upon complementation with peptide C10. In Scheme II, the guanidine hydrochloride-denatured bpDNase was not able to refold back to the correct conformation in the absence of Ca^{2+}, and this misfolded protein was inactive. Again, addition of Ca^{2+} facilitated the refolding of the misfolded protein to the nativelike structure with full regain of DNase activity. When the C-terminal deletion variant [brDNase(Δ251−260)] in 6 M guanidine hydrochloride was dialyzed in a Ca^{2+}-containing buffer, it formed a partially folded structure rich in α-helix first and slowly folded to the mainly β-sheet structure upon complementation with peptide C10 (Scheme III). Likewise, when the guanidine hydrochloride-denatured bpDNase was dialyzed against a Ca^{2+}-containing buffer, the unfolded protein could be refolded back to the nativelike structure with full DNase activity (Scheme IV).

One large "essential" disulfide loop (C173−C209) and one small "nonessential" disulfide bond (C101−C104) were previously studied for their involvements in the bpDNase activities, and the reduction of the essential disulfide could result in the complete loss of DNase activity (*23*). In the present study, because there were no dimers or higher oligomers formed in all of the active and inactive variants, as shown on SDS−PAGE under nonreducing conditions (Figure 3), brDNase variants with full DNase activities were presumed to have correctly paired intrachain disulfide bonds similar to those in native bpDNase. For the inactive variants (mostly unfolded), whether the loss of the activity was due to the mispairing of the disulfides was unclear.

Earlier studies on bpDNase (*6*) have shown that the intact C-terminus is crucial for the active conformation of the enzyme. It was accessible to carboxypeptidase A only after denaturation by 0.005% SDS, and removal of Thr260 and Leu259 thereafter by carboxypeptidase A led to almost complete inactivation of the enzyme. Although several hydrogen-bonding contacts were observed in the residue, Thr260, resulting in inaccessibility to carboxypeptidase A, its removal did not affect the activity as shown in the brDNase(Δ260) variant. However, deletion of one more amino acid residue, as in the brDNase(Δ259−260) variant, produced a completely inactive protein. These observations can be rationalized by the fact that the next amino acid residue, Leu259, is part of sheet 1 (*2*) and its removal would disrupt the hydrogen bonding in the center of this sheet (between strands A and P) and thereby destabilize the structure. Therefore, these results further support the hypothesis that the C-terminal motif is critical to the active protein folding of bpDNase by forming the antiparallel β-sheet structure with the N-terminal motif.

An *E. coli* RNase H variant lacking the C-terminal E-helix folded cooperatively as a subdomain and retained a weak Mn^{2+}-dependent activity (*27*). A peptide corresponding to the deleted E-helix was intrinsically helical and stimulated the activity of the deletion variant with a K_d of 50 μM. Moreover, studies have also shown that a variant deleted of the 12 C-terminal residues of yeast phosphoglycerate kinase folded in a conformation very similar to that of the wild-type protein but exhibited a very low activity. The addition of the missing peptide provoked a 40-fold increase in enzyme activity at saturation, with a K_d of 80 μM determined (*28*). In our present studies, peptide C10 interacting with the brDNase(Δ251−260) variant yielded a K_d of 48 μM, comparable to the values obtained in the peptide complementation studies of RNase H and phosphoglycerate kinase.

bpRNase A, in which 4−9 C-terminal amino acid residues were removed, had as much as 90% RNase activity reactivated by admixing with C-terminal peptides of 9−14 residues (*29*−*33*). bpDNase, where 2−6 C-terminal residues were removed by carboxypeptidase A, regenerated only about 2% DNase activities upon incubation with a 15-residue C-terminal peptide (*6*). In the present study, we improved the

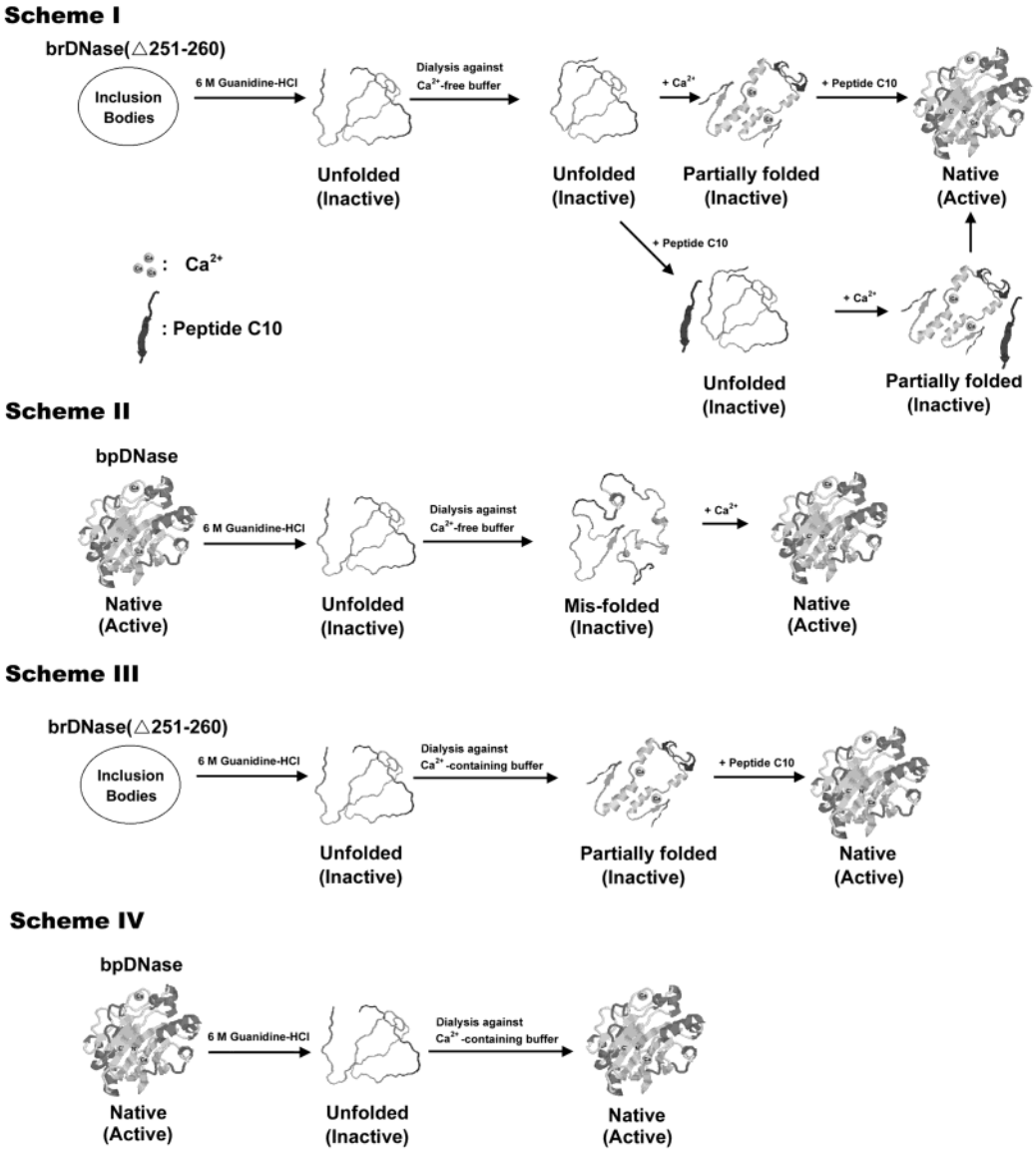

FIGURE 9: Schemes illustrating the roles of Ca^{2+} in the folding activation of the deletion variant, brDNase(Δ251−260), complemented with peptide C10 and in the refolding reactivation of the guanidine hydrochloride-denatured bpDNase.

experiment in bpDNase by using the C-terminal deletion variants complemented with synthetic peptides. Almost a full activation was observed by the complementation of brDNase-(Δ251−260) with peptide C10 and by the complementation of brDNase(Δ1−11) with peptide N10 (Figure 5 and Table 2). The results suggested that the subdomain of the deletion variants maintained affinity for the complementary peptides. Peptide C10A, very similar to peptide C10, in which the catalytically essential His252 was replaced by alanine, could also facilitate brDNase(Δ251−260) to fold into a nativelike β-sheet-rich structure, but it failed to activate the deletion variant (Table 2), indicating that this type of peptide interaction possessed a certain degree of specificity.

Thornton and Sibanda (*34*) have pointed out that the N- and C-terminal regions in globular proteins are often located in close proximity and are less frequently involved in activity but fulfill a structural role by stabilizing the tertiary structure to provide a framework for the active site. The C-terminal motif of yeast phosphoglycerate kinase was not necessary for most of the initial folding steps except to lock the C-domain on the N-domain, thus ensuring the expression of full enzyme activity (*28*). However, side-chain packing of the N- and C-terminal helices was a critical early event in the folding of cytochrome *c* and was responsible for the formation of a partially folded intermediate (*35*). The N- and C-terminal fragments of bpDNase are in close proximity, and the main-chain hydrogen bonding in the N- and C-terminal antiparallel β-sheet structure was found to be crucial for achieving the efficient packing into its active conformation, as shown in the deletion and substitution variants (Figures 3).

A protein must be folded to be functional following its biosynthesis on the ribosome. A newly synthesized polypeptide that converts itself into a uniquely folded structure, depending on the amino acid sequence, and has the ability to perform an enzymatic function by changing random molecular motion into a self-organized protein structure is therefore an evolutionary result. The C-terminal residues are the last to be added in the protein biosynthetic pathway, and in many instances they have a determining role in the active protein folding. Thus, the C-terminal region often participates in protein folding, structural stability, and in some cases

enzymatic activity as shown in ribonuclease A (*29*−*33*), ribonuclease H (*27*), ribonuclease S (*36*), staphylococcal nuclease (*37*), phosphoglycerate kinase (*28*), cytochrome *c* (*35*), glutathione transferase (*38*), creatine kinase (*39*), thymidylate synthetase (*40*), and lipase (*41*). Furthermore, the C-terminal residues may be involved in chaperone activity and oligomerization. For example, C-terminal truncation variants of αA-crystallin were found in diabetic rat and human lenses with their chaperone activity severely affected (*42*), and a C-terminal deletion of neuronal α-synuclein led to the facilitated aggregation with the elimination of chaperone activity, resulting in the pathogenesis of Parkinson's disease (*43*). In the present study, we addressed the importance of the C-terminal motif in the active folding of bpDNase using a deletion variant complemented with a peptide corresponding to the deleted portion of the C-terminus and in the participation of His252 at the active site.

The circularly permuted proteins, which arose through the ligation of the N- and C-termini and the subsequent cleavage at another site to produce new termini, have been demonstrated (*44*). These permuted proteins often folded into stable, functional conformations, very similar to the native protein, albeit at slower rates. The circularly permuted proteins have also been reported to occur naturally (*45*) at the level of posttranslational modifications or events at the gene level, although it is improbable that circular permutations will prove to be a very frequent event in the evolution of protein genes. A prerequisite for the formation of a circularly permuted protein was the proximity of the N- and C-termini in the folded protein domain. In our present study, the N- and C-termini of bpDNase, though located in close proximity similar to those of the circularly permuted proteins, were proved to play a determining role in the active protein folding by antiparallel β-sheet formation.

The existence of partially folded intermediates may be essential for proteins to fold in a biologically meaningful time scale. Although partially folded intermediates have been observed in larger proteins, they are generally not detectable in the kinetic folding of smaller proteins. Recent native state hydrogen-exchange studies suggest that partially folded intermediates, escaping detection by conventional kinetic methods, may exist behind the rate-limiting transition state in small proteins. Hydrogen-exchange experiments showed that cytochrome *c* (*46*) under native conditions reversibly unfolded in a multistep manner. The step from one intermediate to the next is determined by the intrinsically cooperative nature of secondary structural elements, which is retained in the sequence of the protein. Folding uses the same pathway in the reverse direction, moving from the unfolded to the native state through relatively discrete intermediates by the sequential addition of nativelike secondary structural units. Studies have also shown that some species can have extensive nativelike secondary structure in the absence of well-defined tertiary interactions. These species are frequently known as molten globules (*47*). For a number of proteins, similar species have been found to be stable at equilibrium under mild denaturing conditions, such as acidic pH values or low concentrations of guanidine hydrochloride (*48*, *49*). As evidenced by the peptide complementation (Figure 5) and CD (Figures 6 and 8) studies, the folding activation process of the C-terminal deletion variant, brDNase(Δ251−260), occurred in two stages. The first stage was the folding associated with Ca^{2+} binding for acquisition of a partially folded intermediate with mainly helical structures. The second stage was the formation of a structure rich in β-sheet upon peptide C10 binding followed by a tight packing of the preformed secondary structure segments to lead to the final native structure through the formation of the N- and C-terminal antiparallel β-sheets.

The fact that the Ca^{2+}-induced conformational changes are slow (*25*) may explain the slow activation of the deletion variant by the complementary peptide. Results from the slow dissociation rate for the brDNase(Δ251−260) variant−peptide C10 complex (Figure 5C) also provided evidence that once the complex was formed, the N- and C-terminal antiparallel β-sheet structure was tightly packed as shown by the increase in T_m (Figure 7). Thus, Ca^{2+} participates in the folding activation process of the deletion variant (Figure 9) by stabilizing the partially folded species, facilitating the formation of the N- and C-terminal antiparallel β-sheets, and enabling the efficient conversion of the polypeptide into its packed native structure.

ACKNOWLEDGMENT

We thank Dr. Lu-Ping Chow for protein sequencing.

SUPPORTING INFORMATION AVAILABLE

Sequences of the oligonucleotides used for construction of various brDNase variants (Table S1). This material is available free of charge via the Internet at http://pubs.acs.org.

REFERENCES

1. Moore, S. (1981) Pancreatic DNase, in *The Enzymes* (Boyer, P. D., et al., Eds.) 3rd ed., Vol. 14, pp 281−296, Academic Press, New York.
2. Suck, D., Oefner, C., and Kabsch, W. (1984) Three-dimensional structure of bovine pancreatic DNase I at 2.5 Å resolution, *EMBO J. 3*, 2423−2430.
3. Oefner, C., and Suck, D. (1986) Crystallographic refinement and structure of DNase I at 2 Å resolution, *J. Mol. Biol. 192*, 605−632.
4. Chen, W. J., Lee, I. S., Chen, C. Y., and Liao, T. H. (2004) Biological functions of the disulfides in bovine pancreatic deoxyribonuclease, *Protein Sci. 13*, 875−883.
5. Chen, C. Y., Lu, S. C., and Liao, T. H. (2002) The distinctive functions of the two structural calcium atoms in bovine pancreatic deoxyribonuclease, *Protein Sci. 11*, 659−668.
6. Liao, T. H. (1975) Reversible inactivation of pancreatic deoxyribonuclease A by sodium dodecyl sulfate: removal of COOH-terminal residues from the denatured protein by carboxypeptidase A, *J. Biol. Chem. 250*, 3831−3836.
7. Paudel, H. K., and Liao, T.-H. (1986) Comparison of the three primary structures of deoxyribonuclease isolated from bovine, ovine, and porcine pancreas. Derivation of the amino acid sequence of ovine DNase and revision of the previously published amino acid sequence of bovine DNase, *J. Biol. Chem. 261*, 16012−16017.
8. Kaneko, Y., Takeshita, H., Mogi, K., Nakajima, T., Yasuda, T., Itoi, M., Kuwano, H., and Kishi, K. (2003) Molecular, biochemical and immunological analyses of canine pancreatic DNase I, *J. Biochem. 134*, 711−718.
9. Polzar, B., and Mannherz, H. G. (1990) Nucleotide sequence of a full length cDNA clone encoding the deoxyribonuclease I from the rat parotid gland, *Nucleic Acids Res. 18*, 7151.
10. Peitsch, M. C., Irmler, M., French, L. E., and Tschopp, J. (1995) Genomic organization and expression of mouse deoxyribonuclease, *Biochem. Biophys. Res. Commun. 207*, 62−68.
11. Hu, C. C., Lu, S. C., Cheng, C. C., Chen, L. H., and Liao, T. H. (2003) Chicken deoxyribonuclease: purification, characterization, gene cloning and gene expression, *J. Protein Chem. 22*, 41−49.

12. Takeshita, H., Yasuda, T., Nakajima, T., Mogi, K., Kaneko, Y., Iida, R., and Kishi, K. (2003) A single amino acid substitution of Leu120Ile in snake DNases I contributes to the acquisition of thermal stability. A clue to the molecular evolutionary mechanism from cold-blooded to warm-blooded vertebrates, *Eur. J. Biochem. 270*, 307−314.
13. Takeshita, H., Yasuda, T., Iida, R., Nakajima, T., Mori, S., Mogi, K., Kaneko, Y., and Kishi, K. (2001) Amphibian DNases I are characterized by a C-terminal end with a unique, cysteine-rich stretch and by the insertion of a serine residue into the Ca^{2+}-binding site, *Biochem. J. 357*, 473−480.
14. Landt, O., Grunert, H. P., and Hahn, U. (1990) A general method for rapid site-directed mutagenesis using the polymerase chain reaction, *Gene 96*, 125−128.
15. Laemmli, U. K. (1970) Cleavage of structural proteins during the assembly of the head of bacteriophage T4, *Nature 227*, 680−685.
16. Merril, C. R., Goldman, D., Sedman, S. A., and Ebert, M. H. (1981) Ultrasensitive stain for proteins in polyacrylamide gels shows regional variation in cerebrospinal fluid proteins, *Science 211*, 1437−1438.
17. Liao, T. H. (1974) Bovine pancreatic deoxyribonuclease D, *J. Biol. Chem. 249*, 2354−2356.
18. Bradford, M. M. (1976) A rapid and sensitive method for the quantitation of microgram quantities of protein utilizing the principle of protein-dye binding, *Anal. Biochem. 72*, 248−254.
19. Wu, C. S., Ikeda, K., and Yang, J. T. (1981) Ordered conformation of polypeptides and proteins in acidic dodecyl sulfate solution, *Biochemistry 20*, 566−570.
20. Chen, Y. H., Yang, J. T., and Chau, K. H. (1974) Determination of the helix and beta form of proteins in aqueous solution by circular dichroism, *Biochemistry 13*, 3350−3359.
21. Jones, S. J., Worrall, A. F., and Connolly, B. A. (1996) Site-directed mutagenesis of the catalytic residues of bovine pancreatic deoxyribonuclease I, *J. Mol. Biol. 264*, 1154−1163.
22. Liao, T. H., Ho, H. C., and Abe, A. (1991) Chemical modification of bovine pancreatic deoxyribonuclease with phenylglyoxal—the involvement of Arg-9 and Arg-41 in substrate binding, *Biochim. Biophys. Acta 1079*, 335−342.
23. Price, P. A., Stein, W. H., and Moore, S. (1969) Effect of divalent cations on the reduction and re-formation of the disulfide bonds of deoxyribonuclease, *J. Biol. Chem. 244*, 929−932.
24. Price, P. A., Liu, T.-Y., Stein, W. H., and Moore, S. (1969) Properties of chromatographically purified bovine pancreatic deoxyribonuclease, *J. Biol. Chem. 244*, 917−923.
25. Poulos, T. L., and Price, P. A. (1972) Some effects of calcium ions on the structure of bovine pancreatic deoxyribonuclease A, *J. Biol. Chem. 247*, 2900−2904.
26. Lizarraga, B., Sanchez-Romero, D., Gil, A., and Melgar, E. (1978) The role of Ca^{2+} on pH-induced hydrodynamic changes of bovine pancreatic deoxyribonuclease A, *J. Biol. Chem. 253*, 3191−3195.
27. Goedken, E. R., Raschke, T. M., and Marqusee, S. (1997) Importance of the C-terminal helix to the stability and enzymatic activity of *Escherichia coli* Ribonuclease H, *Biochemistry 36*, 7256−7263.
28. Ritco-Vonsovici, M., Mouratou, B., Minard, P., Desmadril, M., Yon, J. M., Andrieux, M., Leroy, E., and Guittet, E. (1995) Role of the C-terminal helix in the folding and stability of yeast phosphoglycerate kinase, *Biochemistry 34*, 833−841.
29. Lin, M. C., Gutte, B., Moore, S., and Merrifield, R. B. (1970) Regeneration of activity by mixture of ribonuclease enzymically degraded from the COOH terminus and a synthetic COOH-terminal tetradecapeptide, *J. Biol. Chem. 245*, 5169−5170.
30. Lin, M. C., Gutte, B., Caldi, D. G., Moore, S., and Merrifield, R. B. (1972) Reactivation of des(119−124) ribonuclease A by mixture with synthetic COOH-terminal peptides; the role of phenylalanine-120, *J. Biol. Chem. 247*, 4768−4774.
31. Gutte, B., Lin, M. C., Caldi, D. G., and Merrifield, R. B. (1972) Reactivation of des(119-, 120-, or 121-124) ribonuclease A by mixture with synthetic COOH-terminal peptides of varying lengths, *J. Biol. Chem. 247*, 4763−4767.
32. Hayashi, R., Moore, S., and Merrifield, R. B. (1973) Preparation of pancreatic ribonuclease 1−114 and 1−115 and their reactivation by mixture with synthetic COOH-terminal peptides, *J. Biol. Chem. 248*, 3889−3892.
33. Fujii, T., Ueno, H., and Hayashi, R. (2002) Significance of the four carboxyl terminal amino acid residues of bovine pancreatic ribonuclease A for structural folding, *J. Biochem. 131*, 193−200.
34. Thornton, J. M., and Sibanda, B. L. (1983) Amino and carboxy-terminal regions in globular proteins, *J. Mol. Biol. 167*, 443−460.
35. Colon, W., Elove, G. A., Wakem, L. P., Sherman, F., and Roder, H. (1996) Side chain packing of the N- and C-terminal helices plays a critical role in the kinetics of cytochrome *c* folding, *Biochemistry 35*, 5538−5549.
36. Goldberg, J. M., and Baldwin, R. L. (1999) A specific transition state for S-peptide combining with folded S-protein and then refolding, *Proc. Natl. Acad. Sci. U.S.A. 96*, 2019−2024.
37. Hirano, S., Mihara, K., Yamazaki, Y., Kamikubo, H., Imamoto, Y., and Mikio, K. (2002) Role of C-terminal region of *Staphylococcal* nuclease for foldability, stability, and activity, *Proteins 49*, 255−265.
38. Dirr, H. W., and Wallace, L. A. (1999) Role of the C-terminal helix 9 in the stability and ligandin function of class α glutathione transferase A1-1, *Biochemistry 38*, 15631−15640.
39. Mazon, H., Marcillat, O., Vial, C., and Clottes, E. (2002) Role of C-terminal sequences in the folding of muscle creatine kinase, *Biochemistry 41*, 9646−9653.
40. Hazebrouck, S., Maley, F., Machtelinckx, V., Sonigo, P., and Kupiec, J. J. (1999) Structural and functional analysis of surface domains unique to bacteriophage T4 thymidylate synthase, *Biochemistry 38*, 2094−2101.
41. Jennens, M. L., and Lowe, M. E. (1995) C-terminal domain of human pancreatic lipase is required for stability and maximal activity but not colipase reactivation, *J. Lipid Res. 36*, 1029−1036.
42. Thampi, P., and Abraham, E. C. (2003) Influence of the C-terminal residues on oligomerization of αA-crystallin, *Biochemistry 42*, 11857−11863.
43. Kim, T. D., Paik, S. R., and Yang, C.-H. (2002) Structural and functional implications of C-terminal regions of α-synuclein, *Biochemistry 41*, 13782−13790.
44. Luger, K., Hommel, U., Herold, M., Hofsteenge, J., and Kirschner, K. (1989) Correct folding of circularly permuted variants of a beta alpha barrel enzyme in vivo, *Science 243*, 206−210.
45. Lindqvist, Y., and Schneider, G. (1997) Circular permutations of natural protein sequences: structural evidence, *Curr. Opin. Struct. Biol. 7*, 422−427.
46. Krishna, M. M., Lin, Y., Mayne, L., and Englander, W. S. (2003) Intimate view of a kinetic protein folding intermediate: residue-resolved structure, interactions, stability, folding and unfolding rates, homogeneity, *J. Mol. Biol. 334*, 501−513.
47. Ptitsyn, O. B. (1995) Structures of folding intermediates, *Curr. Opin. Struct. Biol. 5*, 74−78.
48. Dobson, C. M. (1995) Finding the right fold, *Nat. Struct. Biol. 2*, 513−517.
49. Kuwajima, K., Mitani, M., and Sugai, S. (1989) Characterization of the critical state in protein folding. Effects of guanidine hydrochloride and specific Ca^{2+} binding on the folding kinetics of alpha-lactalbumin, *J. Mol. Biol. 206*, 547−561.
50. Shak, S., Capon, D. J., Hellmiss, R., Marsters, S. A., and Baker, C. L. (1990) Recombinant human DNase I reduces the viscosity of cystic fibrosis sputum, *Proc. Natl. Acad. Sci. U.S.A. 87*, 9188−9192.
51. Yasuda, T., Takeshita, H., Nakajima, T., Hosomi, O., Nakashima, Y., and Kishi, K. (1997) Rabbit DNase I: purification from urine, immunological and proteochemical characterization, nucleotide sequence, expression in tissues, relationships with other mammalian DNases I and phylogenetic analysis, *Biochem. J. 325*, 465−473.
52. Hsiao, Y. M., Ho, H. C., Wang, W. Y., Tam, M. F., and Liao, T. H. (1997) Purification and characterization of tilapia (*Oreochromis mossambicus*) deoxyribonuclease I—primary structure and cDNA sequence, *Eur. J. Biochem. 249*, 786−791.
53. Lacks, S. A., Springhorn, S. S., and Rosenthal, A. L. (1979) Effect of the composition of sodium dodecyl sulfate preparations on the renaturation of enzymes after polyacrylamide gel electrophoresis, *Anal. Biochem. 100*, 357−363.

BI049183I